Supplementary Information

The Condensed-phase Optimized Molecular Potentials for Atomistic Simulation Studies (COMPASS) force field:

$$E = \sum_{b}\left[K_2(b-b_0)^2 + K_3(b-b_0)^3 + K_4(b-b_0)^4\right] \quad (i)$$

$$+ \sum_{\theta}\left[H_2(\theta-\theta_0)^2 + H_3(\theta-\theta_0)^3 + H_4(\theta-\theta_0)^4\right] \quad (ii)$$

$$+ \sum_{\emptyset}\left\{V_1\left[1-cos\left(\emptyset-\emptyset_1{}^0\right)\right] + V_2\left[1-cos\left(\emptyset-2\emptyset_2{}^0\right)\right] + V_3\left[1-cos\left(\emptyset-3\emptyset_3{}^0\right)\right]\right\} \quad (iii)$$

$$+ \sum_{x}K_x x^2 + \sum_{b}\sum_{b'}F_{bb'}(b-b_0)\left(b'-b'_0\right) + \sum_{\theta}\sum_{\theta'}F_{\theta\theta'}(\theta-\theta_0)\left(\theta'-\theta'_0\right)$$

(iv) (v) (vi)

$$+ \sum_{b}\sum_{\theta}F_{b\theta}(b-b_0)(\theta-\theta_0) + \sum_{b}\sum_{\emptyset}(b-b_0)[V_1 cos\emptyset + V_2 cos2\emptyset + V_3 cos3\emptyset]$$

(vii) $(viii)$

$$+ \sum_{b'}\sum_{\theta}F_{b\theta}\left(b'-b'_0\right) + [V_1 cos\emptyset + V_2 cos2\emptyset + V_3 cos3\emptyset] \quad (ix)$$

$$+ \sum_{\emptyset}\sum_{\theta}\sum_{\theta'}K_{\emptyset\theta\theta'}cos\emptyset(\theta-\theta_0)\left(\theta'-\theta'_0\right) + \sum_{i>j}\frac{q_i q_j}{r_{ij}} + \sum_{i>j}\varepsilon_{ij}\left[2\left(\frac{\sigma_{ij}}{r_{ij}}\right)^9 - 3\left(\frac{\sigma_{ij}}{r_{ij}}\right)^6\right] \quad (S1)$$

(x) (xi) (xii)

In COMPASS, the energy term, E, has been characterized via three major categories, which are namely: (a) the bonded energy (b) the cross-terms and (c) the non-bonded energy contributions. The bonded energy is consisted of contributions (i) – (iv) in (S1) such as the following, (i) the covalent bond stretching energy terms (ii) the bond angle bending energy terms (iii) the torsion angle rotation energy terms of the polymeric chains, which has been fitted by a Fourier series function readily available in the software and (iv) the out-of-plane energy or improper term that has been described as a harmonic function. On the other hand, the cross interaction contribution is constituted through the (v) – (x) terms in (8), which encompass the characterization of dynamic variation among bond stretching, bending, and torsion angle rotation. Finally, the last two terms, (xi) and (xii), which are representative terms of the non-bonded energy that illustrate the interactive forces between polymer chains

and small molecules, describe the Columbic electrostatic force and van der Waals interaction respectively [1]. Detail description pertaining to the energy contributions can be found elsewhere in published literature [2, 3] and within Materials Studio itself [4].

For the non-bonded Lennard Jones energy term, it has been described with a sixth-order combination rule in order to calculate the corresponding parameters, such as that provided in (S2) and (S3).

$$\sigma_{ij} = \left(\frac{\sigma_i^{\,6} + \sigma_j^{\,6}}{2}\right)^{\frac{1}{6}} \qquad (S2)$$

$$\varepsilon_{ij} = 2\sqrt{\varepsilon_i \varepsilon_j}\left(\frac{\sigma_i^{\,3}\sigma_i^{\,3}}{\sigma_i^{\,6} + \sigma_i^{\,6}}\right) \qquad (S3)$$

In (S2) and (S3), σ_{ij} is the distance at which the potential energy is zero, ε_{ij} corresponds to the well-depth of the interaction potential, while σ_i and ε_i represent the size and energy parameters of the interaction atoms respectively, which are commonly known as the Lennard Jones parameters. As for the Columbic electrostatic term, the partial charges are computed from the charge bond increment, δ_{ij}, which represents charge separation between two valence-bonded atoms [3, 5]. The net charge, q_i, for atom i is a summation of all charge bond increments related to atom i, such as that depicted in (S4).

$$q_i = \sum_j \delta_{ij} \qquad (S4)$$

Cavity Energetic Sizing Algorithm [6]. Symbols are provided in the Abbreviation section.

(1)

$$\varphi_t' = 4\sum_{i=1}^{N}\varepsilon_{ti}\left(\frac{\sigma_{ti}}{r_{ti}}\right)^{12} \quad (S5)$$

$$\sigma_{ti} = \frac{1}{2}(\sigma_t + \sigma_i) \quad (S6)$$

$$\varepsilon_{ti} = \sqrt{\varepsilon_t \varepsilon_i} \quad (S7)$$

$$r_{ti} = |\vec{r}_t - \vec{r}_i| \quad (S8)$$

Pure repulsive force field has been activated based on modified Lennard Jones 12-6 potential in (S5), effective parameters are obtained from arithmetic and geometric mean in (S6) and (S7). Expression (S8) depicts the distance between the test particle and atom.

(2)

$$\nabla ln(\varphi_t) = \frac{\nabla \varphi_t'}{\quad} = -\frac{48}{\quad}\sum^{N} \varepsilon_{ti}\frac{r_{ti}}{\quad 2}\left(\frac{\sigma_{ti}}{r}\right)^{12} (S9)$$

Multivariable Newton method combined with steepest descent method to locate the position of local min for test particles, as demonstrated in (S9).

(3)

$$\varphi_t = 4\left[\sum_{i=1}^{N}\varepsilon_{ti}\left(\frac{\sigma_{ti}}{r_{ti}}\right)^{12} - \left(\frac{\sigma_{ti}}{r_{ti}}\right)^{6}\right] (S10)$$

Attractive force field has been turned on, which is the conventional 6-12 Lennard Jones Potential Equation, as shown in (S10).

(4) $\varphi_t = 0$ $(S11)$

Size of the trial particle has been adjusted until its potential interaction with all neighboring atoms approaches zero, whereby the criterion for convergence is depicted in (S11).

(5)

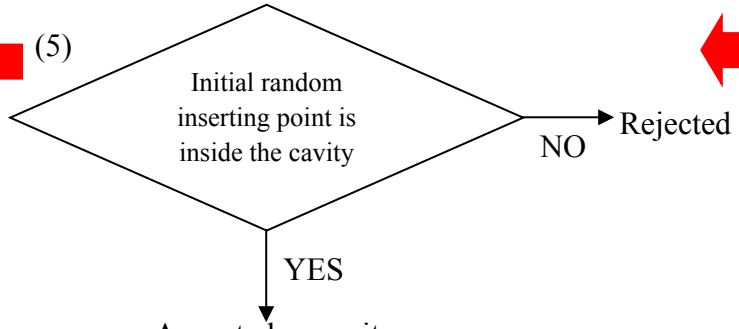

(6) Iteration to obtain cavity distribution

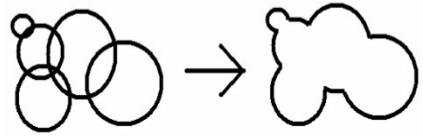

Overlapping cavities are merged to form cluster

Figure S 1 Chronological development and fundamental theory underlying the CESA to determine cavity distribution of PSF polymeric membranes of varying thicknesses, adapted from In't Veld (2000) [6]

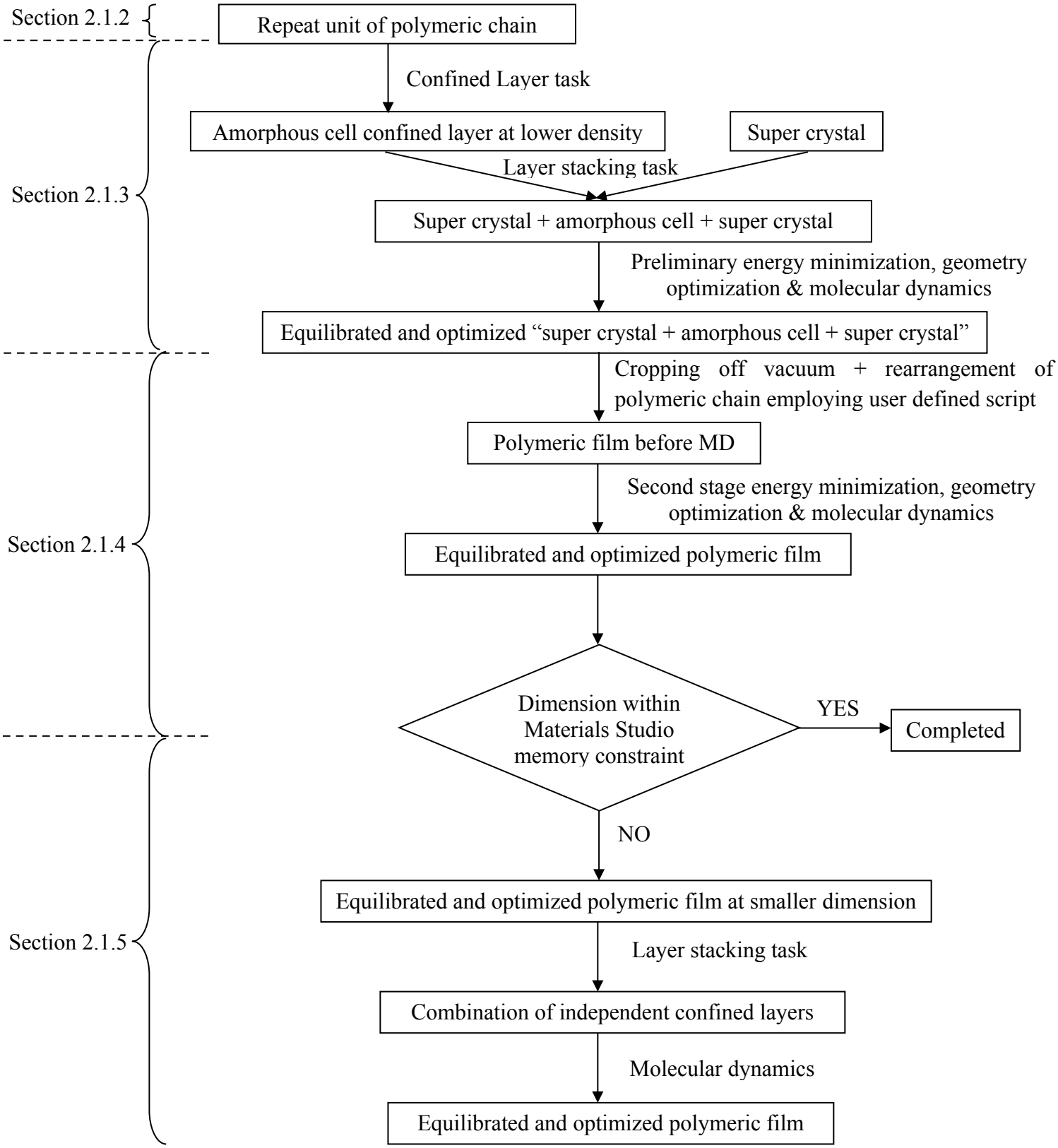

Figure S 2 Overview and chronological development in the Soft Confining Methodology for Ultrathin Films

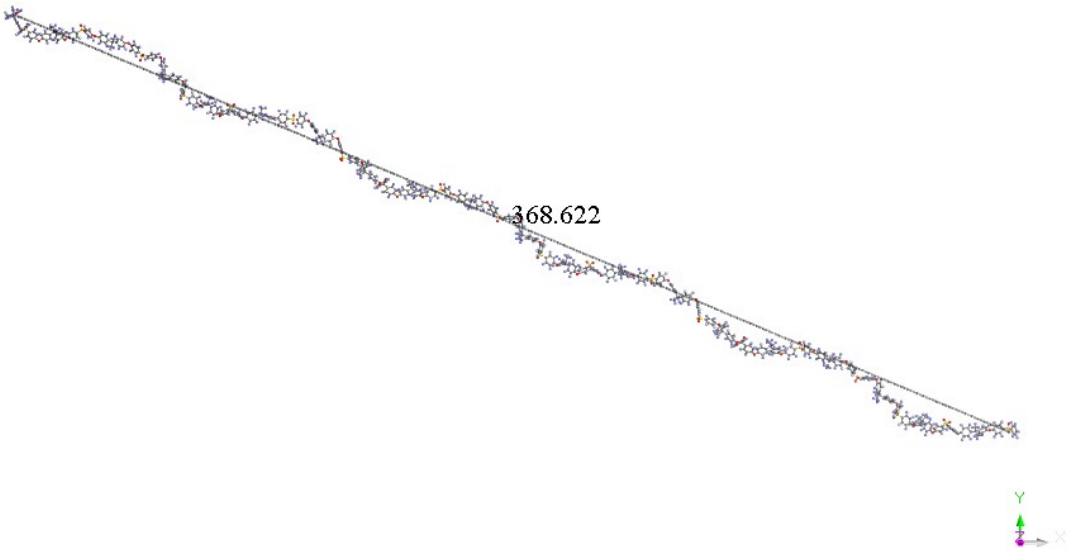

Figure S 3 Chain end-to-end distance of PSF chain initial configuration before molecular modelling treatment

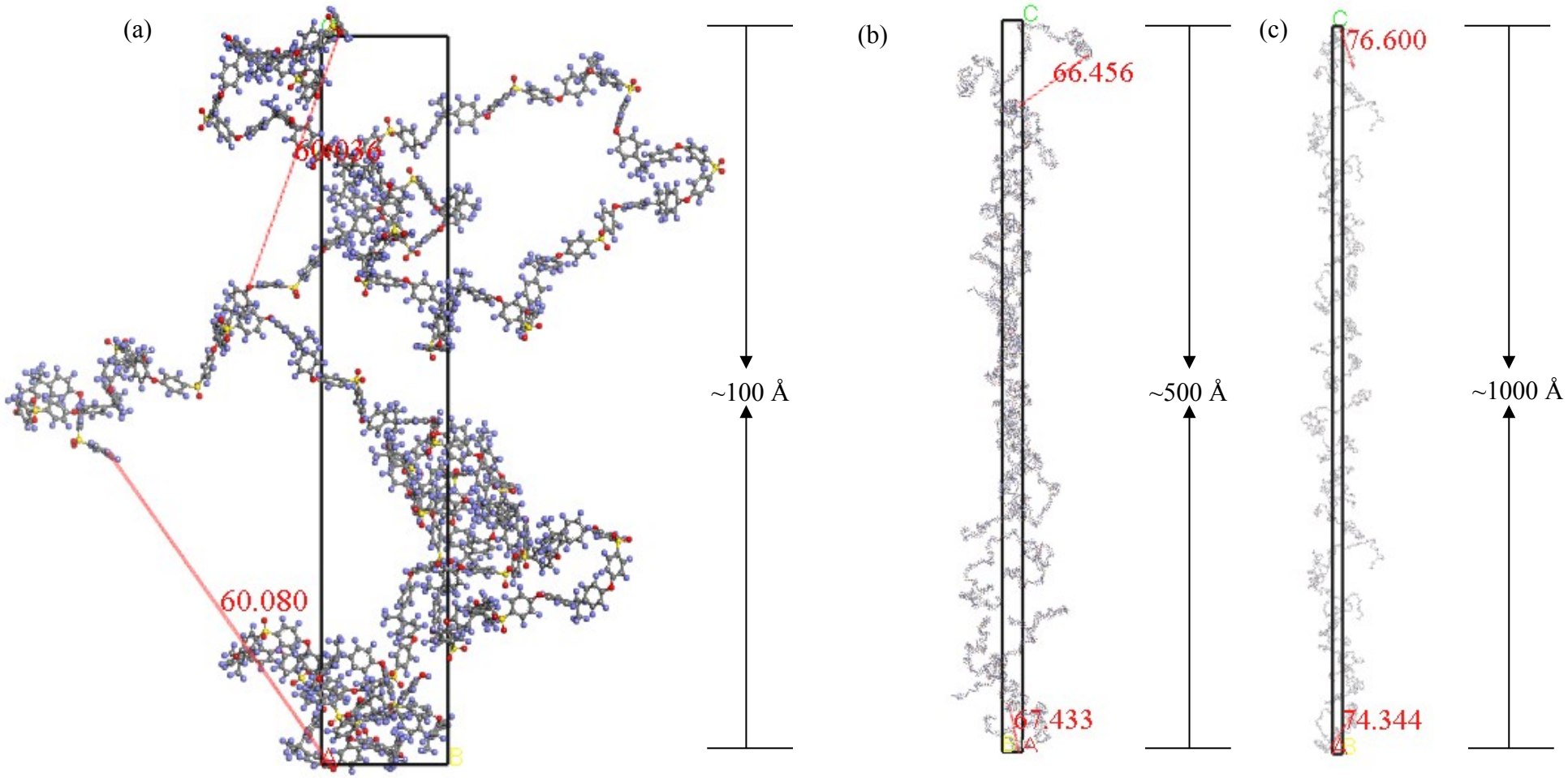

Figure S 4 Chain end-to-end-distance of final configuration in PSF polymeric membrane films of a) ~100 Å (16.03×16.03×91.87) b) ~500 Å (15.17×15.17×515.68) and c) ~1000 Å (15.32×15.32×1026.79). Default view" within Materials Studio has been provided, whereby molecules are translated so that their centres of geometry are located in the simulation cell. Lines denote periodic boundary condition conditions in both the x and y directions, while z direction characterizes thickness of the polymeric film (The chain end-to-end distance of two PSF polymeric chains have been provided as examples for each thickness to guide readers)

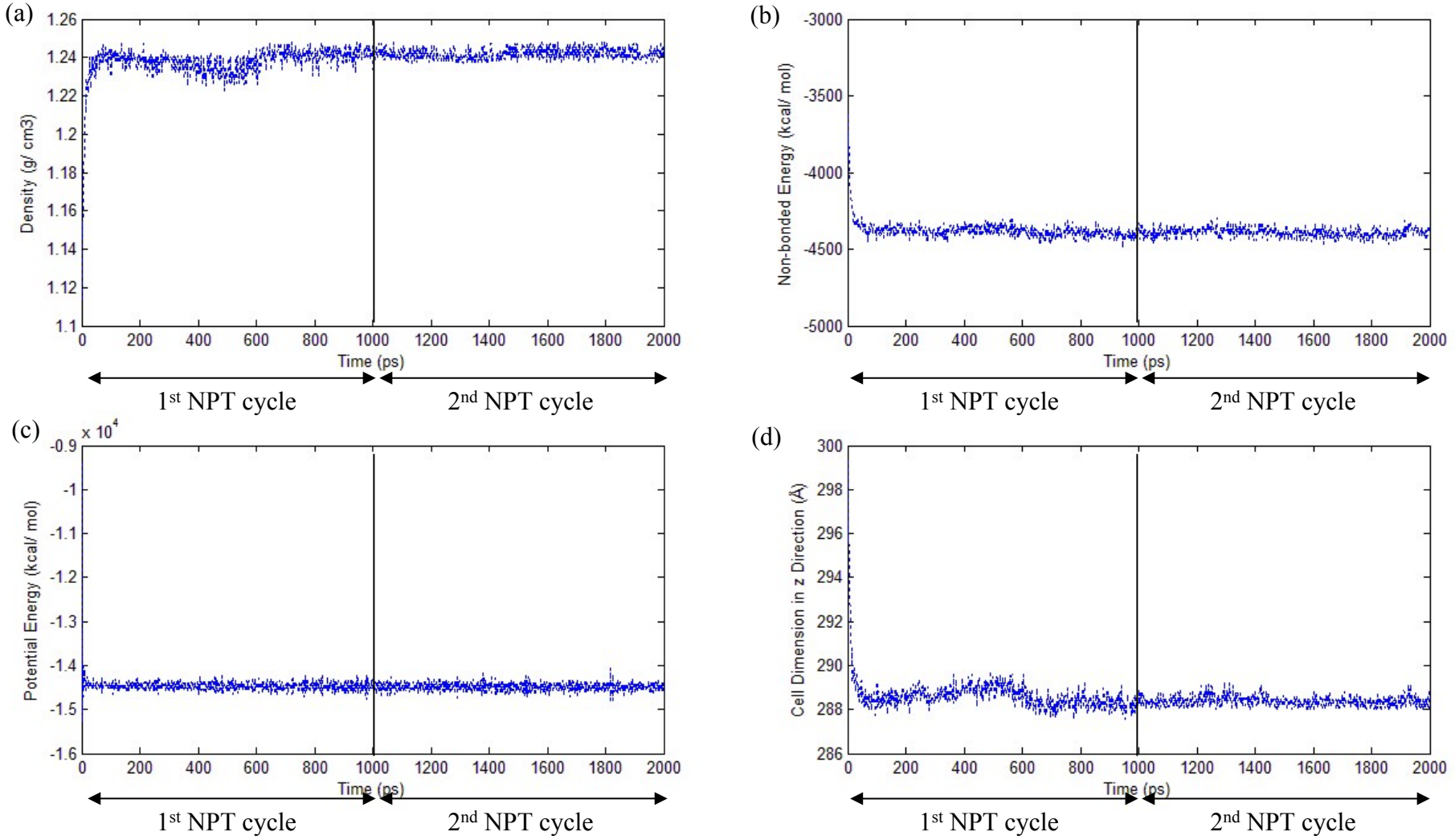

Figure S 5 Evolution change during molecular dynamics simulation for a) Density b) Non-bonded energy c) Potential energy and d) Cell dimension in PSF with ~300 Å obtained via combination of three ~100 Å structures via the layer to layer methodology

(Example of two cycles 1000 ps NPT molecular treatment has been provided)

Abbreviation

$\varphi_t^{'}$	Pure repulsive force field based on modified Lennard Jones (LJ) 12-6 potential, which characterizes the interaction energy of the test particle with the other i particles
ε_{ti}	Depth of the potential well of test particle with the other i particles
ε_i	LJ parameter that characterizes depth of potential well of particle i
ε_t	LJ parameter that characterizes depth of potential well of test particle
σ_{ti}	Finite distance of test particle with the other i particles at which the inter-particle potential is zero
σ_i	LJ parameter that characterizes finite distance of particle i
σ_t	LJ parameter that characterizes finite distance of test particle
r_{ti}	Distance of test particle with the other i particles
$\vec{r}_i$	The position vector of particle i
$\vec{r}_t$	The position vector of test particle
φ_t	Conventional 6-12 Lennard Jones potential, which characterizes the interaction energy of the test particle with the other i particles

References

1. K.-S. Chang, Y.-H. Huang, K.-R. Lee and K.-L. Tung, J. Membr. Sci., 2010, 354, 93-100.
2. H. Sun, P. Ren and J. R. Fried, Comput. Theor. Polym. Sci., 1998, 8, 229-246.
3. H. Sun, J. Phys. Chem. B, 1998, 102, 7338-7364.
4. , Accelrys Software Inc., 2015.
5. J. Yang, Y. Ren, A.-M. Tian and H. Sun, J. Phys. Chem. B, 2000, 104, 4951-4957.
6. P. J. in 't Veld, M. T. Stone, T. M. Truskett and I. C. Sanchez, J. Phys. Chem. B, 2000, 104, 12028-12034.